Composites Science and Technology xxx (2016) xxx-xxx

Contents lists available at ScienceDirect

Composites Science and Technology

journal homepage: www.elsevier.com

Separation of core-shell structured carbon black nanoparticles from waste tires by light pyrolysis

Shuo Li [a], Chaoying Wan [b], Shifeng Wang [a, *], Yong Zhang [a]

[a] Research Institute of Polymer Material, Shanghai Jiao Tong University, Shanghai, 200240, PR China
[b] International Institute for Nanocomposites Manufacturing, WMG, University of Warwick, CV4 7AL, UK

ARTICLE INFO

Article history:
Received 12 June 2016
Received in revised form 7 September 2016
Accepted 8 September 2016
Available online xxx

Keywords:
Waste tires
Core-shell
Carbon black
Separation process
Bound rubber

ABSTRACT

The separation of core-shell structured carbon black (CB_{lp}) nanoparticles from waste tires was investigated by applying a reactive extrusion process. The polymeric shell consisting primarily of crosslinked rubber and loosely bound rubber could be selectively separated by varying the extrusion temperature to 260, 280 and 300 °C. The structure, chemical composition and structure of the separated CB_{lp} were characterized using thermo-gravimetric analysis, X-ray photoelectron spectroscopy, scanning electron microscopy, transmission electron microscopy and dynamic light scattering. The crosslinked structure was persevered in the rubber shell of CB_{lp} after extruding at 260 °C. A layer of loosely bound rubber was observed only in the rubber shell when extruded at 280 °C and 300 °C. The composition of the bound rubber layer is also dependent on the processing temperature.

1. Introduction

There are billions of rubber-based tires that are produced worldwide each year. However, there are still limited sustainable approaches to address the vast amount of waste tires [1–4]. Often, waste tires are buried into landfills as scrap, but these unavoidably cause a series of issues related to environment, economy, land management, health and safety [5,6].

Reclaiming and pyrolysis are regarded as more economical and sustainable methods to dispose of waste tire rubbers compared to landfilling. During the reclaiming process, the covalently crosslinked rubber structure can be destroyed, along with partially broken polymer chains under the combined thermal, mechanical and chemical energy [7,8]. The reclaimed tire rubbers are then re-processable, and can be re-shaped and vulcanized for new products. The reclaiming or devulcanization of tire rubbers is generally performed at elevated temperatures above 200 °C. Lower temperature devulcanization is also attractive because of the reduction of volatile organic compounds (VOC) and less energy consumption [9].

Pyrolysis of waste tires is generally conducted at 400–700 °C in an inert gas atmosphere, which converts rubber tires to activated carbon, pyrolytic carbon black (CB_p), pyro-oil and pyro-gas [10–13]. Undri et al. [14] obtained a relatively small ash content of 5.9–9.5 wt% in the char by using microwave pyrolysis of waste tires. Low temperature pyrolysis could reduce the energy cost but the properties of the reclaimed CB_p were not competitive to those of commercial carbon black [15]. Yamazaki et al. [16] converted waste tires to lower molecular weight (M_n = 10,000) polymers at 300 °C under an air or nitrogen atmosphere. The low molecular weight polymers could be transformed into natural rubber-based grafted copolymers via copolymerization with various vinyl monomers. A twin-screw extrusion at 300 °C [17] was introduced to reclaim waste tires in a continuous, safe and clean process. The reclaimed rubber had a low viscosity, good compatibility with natural rubber, re-crosslinking capability and low cost. Therefore, a processing temperature in the range from 250 °C to 400 °C is feasible to scissor the primary chains of rubbers and largely break the three-dimensional covalent-bonding network of waste tires. However, the emission of VOC is severe at such high temperature, which strictly limits their applicability.

Waste tires are generally composed of styrene-butadiene rubber, butadiene rubber, natural rubber, fillers such as carbon black and silica, curatives, plasticizers and other additives. Bound rubber is a key element in carbon black reinforced tire rubbers. It exists as a complex and stable layer around single particles and agglomerates [21–23], which is formed through the interactions between polymer-polymer and carbon black-polymer during the compounding process [18,19]. The interaction involves physical bonding via van der Waals forces and chemical covalent bonding [20,21]. The bound rubber is composed of two layers [22]and a primary layer including a tightly bound layer and occluded rubber; a secondary layer including connecting filaments. Hoshikawa et al. [24] divided bound rubber into two components: an inner tightly bound rubber layer with a thickness of less than 2 nm and an outer loosely bound rubber layer, which links the carbon black to the rubber matrix [25] (Fig. 1 (a)). The bound rubber-carbon black structure will influence the separation of rubber and carbon black during the pyrolysis of waste tires.

* Corresponding author.
Email address: shfwang@sjtu.edu.cn (S. Wang)

http://dx.doi.org/10.1016/j.compscitech.2016.09.009
0266-3538/

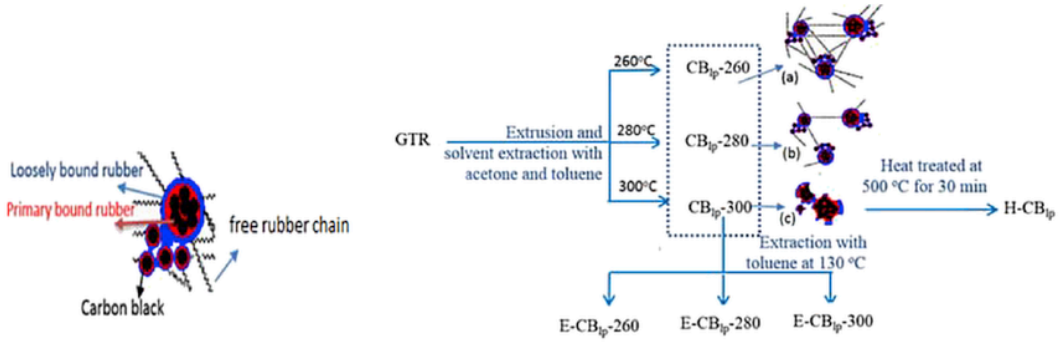

(a) Schematic of original tire rubber (b) Processing procedure of light pyrolysis and separation

Fig. 1. Processing procedure and schematic of CB$_{lp}$-260, CB$_{lp}$-280 and CB$_{lp}$-300.

In this study, lightly pyrolytic carbon black (CB$_{lp}$) was separated from ground tire rubber (GTR) by using a mild twin-extrusion process at three different temperatures (260, 280 and 300 °C), as compared with the conventional pyrolysis process at 400–700 °C. The bound rubber layer was still observed from the surface of CB$_{lp}$ even after the extrusion and solvent extraction processes. The structure and components of the rubber shell were analyzed with thermo-gravimetric analysis (TGA), transmission electron microscopy (TEM) and scanning electron microscopy (SEM). The structure of the core-shell structured CB$_{lp}$ were characterized with X-ray photoelectron spectroscopy (XPS) and dynamic light scattering (DLS). This study unveils the molecular interactions of rubber and carbon black via a thermal degradation approach, and provides potential routes for the recycling and reusing of waste tires.

2. Experimental

2.1. Materials

The ground tire rubber (GTR) (600–700 μm) is shredded and ground at ambient temperature from used whole truck tire rubber by Jiangsu Anqiang Rubber Co., Ltd. The GTR consists of 6.97 wt% soluble material, 40.25 wt% natural rubber, 14.64 wt% synthetic rubber, 30.44 wt% carbon black and 7.70 wt% inorganic filler. The acetone extract content of rubber extruded at 260, 280 and 300 °C is 14.80, 15.50 and 16.30 wt%, respectively. The toluene extraction is 23.80, 28.80 and 36.40 wt%, respectively. The residue after extraction is defined as light pyrolytic carbon black, CB$_{lp}$.

2.2. Preparation

2.2.1. Preparation of CB$_{lp}$

The CB$_{lp}$ was prepared according to the following procedures. First, the GTR was compounded through a reactive extrusion process using a co-rotating inter-meshed twin screw extruder under an air atmosphere (ZE25A from Berstorff GmbH, Germany). The screws had four heating/cooling zones with an L/D ratio of 41 and a diameter of 25 mm. The GTR was added through the hopper at a constant flow rate of (5 kg h^{-1}). The screw rotation speed was set to 300 rpm and the temperature was set at 260, 280 or 300 °C, respectively. The pyrolytic rubber compound was completely dried in an oven at a temperature of 50 °C for 2 h.

Second, 2 g of the pyrolytic rubber compound were extracted with acetone in a Soxhlet extractor at 50 °C for 48 h to remove polar and low-molecular-weight fraction such as accelerators and plasticizers from the rubber. Subsequently, nonpolar components such as soluble rubber were extracted with toluene at 110 °C for 72 h. The residual CB$_{lp}$ was dried in a vacuum oven at 50 °C for 1 h. The acquired samples were denoted as CB$_{lp}$-260, CB$_{lp}$-280 and CB$_{lp}$-300, respectively.

2.2.2. Post-processing of CB$_{lp}$

1) 2 g of CB$_{lp}$-300 was post-heated at 500 °C for 30 min under a nitrogen atmosphere in an electric resistance furnace (SYK-6-14, Shanghai Shiyan Electric Resistance Furnace Works, China), and the obtained sample was denoted as H-CB$_{lp}$.
2) 2 g of samples of CB$_{lp}$-260 CB$_{lp}$-280 and CB$_{lp}$-300 were extracted with toluene at 130 °C for 6 days to remove the rubber chains that were loosely trapped in the bound rubber layer [22]. Then the post-extracted samples were completely dried under vacuum at 50 °C for 24 h, and were denoted as E-CB$_{lp}$-260, E-CB$_{lp}$-280 and E-CB$_{lp}$-300, respectively. The detailed experimental procedures are described in Fig. 1 (b).

2.3. Characterization

The CB$_{lp}$ samples were ultrasonically dispersed in toluene (0.025 g mL^{-1}) and then dropped onto a carbon grid using a micropipette. The grid was dried under vacuum at 50 °C for 24 h and viewed with TEM (JEM-2100, JEOL Ltd., Japan). The well-dispersed CB$_{lp}$ samples in toluene were dropped onto small pieces of silicon sheets and were dried under vacuum at 50 °C for 24 h. The particle size and morphology were observed with SEM (S-2150, Hitachi High-Technologies Corp., Japan).

TGA (Q5000IR, TA Instruments, USA) was used to study the thermal degradation behavior of CB$_{lp}$ and the post-processed CB$_{lp}$. Samples of approximately 5 mg were heated from room temperature to 550 °C under nitrogen protection at a heating rate of 10 °C min^{-1}. Then the samples were heated from 550 °C to 800 °C under oxygen flow with a heating rate of 10 °C min^{-1}.

An XPS analysis was carried out on an AXIS Ultra DLD (Shimadzu, Japan). After ultrasonic dispersion in toluene, the particle sizes of the samples (0.025 g ml^{-1}) were determined using a particle size analyzer ZS90 (Malvern Instruments Ltd., UK) at 25 °C. The Brunauer-Emmett-Teller (BET) surface area of the samples was

tested with an ASAP 2010 M + C (Micromeritics Instrument Corp., USA) with nitrogen as the adsorbate at 100 °C.

Raman analysis was performed with an XYZ multichannel Dispersive Raman Microscope (Senterra R200-L, Bruker Optics Corporation, Germany), employing continuous wave lasers at 532 nm (green) wavelengths. The laser spot size was less than 1 μm, with a spectral resolution less than 1.5 cm^{-1}, and the spectrum was measured in the range of 100–4400 cm^{-1}.

3. Results and discussion

3.1. Morphology of different CB_{lp}

The light pyrolysis carbon black powders were obtained at three different extrusion temperatures (CB_{lp}-260, CB_{lp}-280, and CB_{lp}-300), following the preparation procedure as shown in Fig. 1 (b). The CB_{lp}-260 samples are observed as spongy and bulky agglomerates with a size in the micrometer range as shown in Fig. 2(a). The agglomerates cannot be separated even after extraction with toluene at 130 °C, indicating the coverage of the crosslinked rubber layers on the CB_{lp}-260 surfaces. The CB_{lp}-280, CB_{lp}-300 and H-CB_{lp} are powder-like particles as shown in Fig. 2 (b–d). The particles of CB_{lp}-300 are more uniform in size and evenly distributed as compared to CB_{lp}-260 and CB_{lp}-280. No obvious agglomerates are observed for the H-CB_{lp}.

As characterized by TEM, the primary particles of CB_{lp} are approximately 30 nm in diameter and tend to fuse into carbon black clusters, as shown in Fig. 3. A distinct rubber layer can be observed on the surfaces of both the CB_{lp}-280 and CB_{lp}-300 as shown in Fig. 3(a–b), where the rubber layer of the CB_{lp}-280 is thicker than that of CB_{lp}-300. There is no obvious rubber shell that can be identified from the surface of H-CB_{lp}. This indicates that most of the bound rubber structure might have been destroyed and removed during the thermal treatment at 500 °C for the H-CB_{lp}, which also leads to the reduced size of the H-CB_{lp}, as shown in Fig. 2(d).

3.2. TGA analysis

To understand the composition and thermal stability of CB_{lp}-260, CB_{lp}-280, CB_{lp}-300 and H-CB_{lp}, TGA was used to evaluate the thermal degradation behavior of the materials. As shown in Fig. 4, all of the samples of CB_{lp}-260, CB_{lp}-280, CB_{lp}-300 and H-CB_{lp} exhibit similar thermal degradation behavior at processing temperatures below 300 °C. The distinct thermal weight losses as observed in the temperature range of 350–520 °C and 550–650 °C for CB_{lp}-260, CB_{lp}-280 and CB_{lp}-300 correspond to the decomposition of the rubber shell. The H-CB_{lp} shows only one degradation step at approximately 600 °C indicating that the bound rubber shell on the CB_{lp}-300 surface was removed under the post treatment at 500 °C. The weight loss decreases in the sequence of CB_{lp}-260, CB_{lp}-280 and CB_{lp}-300, indicating the rubber shell content is dependent on the processing temperature. A higher processing temperature removes the loosely bound rubber chains, resulting in a thinner rubber shell structure [26,27]. Therefore, the thermal stability of CB_{lp} is affected by the light pyrolysis temperature.

Table 1 shows the TGA-DTG data for the CB_{lp}-260, CB_{lp}-280 and CB_{lp}-300 samples. The CB_{lp}-300 starts to degrade at T_0 = 339 °C and shows two weight loss peaks with the peak temperatures (T_{max}) at 394 and 494 °C. This can be assigned to the thermal degradation of natural rubber (T_{max1}) and styrene-butadiene rubber (T_{max2}), respectively [7,28,29]. The T_0 and T_{max} of CB_{lp}-300 are higher than the CB_{lp}-260 and CB_{lp}-280 indicating a stronger interfacial interaction between the CB_{lp}-300 particles and rubber shell than those of the CB_{lp}-260 and CB_{lp}-280 [30]. The T_0 and T_{max1} of CB_{lp}-280 are slightly lower than CB_{lp}-260, suggesting that there are free rubber chains connected to the surface of the loosely bound rubber around CB_{lp}-280 [22,24], whose bonding force to carbon black is weaker than the force of the three-dimension network on the surface of CB_{lp}-260.

Bound rubber cannot be extracted by toluene at room temperature, but can be partially removed at 130 °C [22,31]. The CB_{lp} samples were extracted with toluene at 130 °C for 6 days following the procedure in Fig. 1. The content of the rubber shell on the E-CB_{lp} surface were analyzed by TGA, and the results are shown in Fig. 5. The

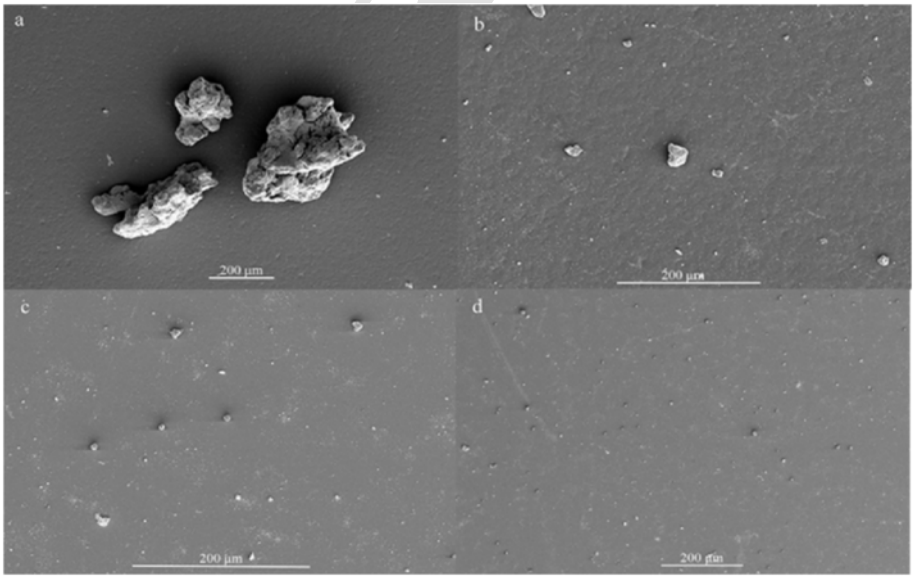

Fig. 2. SEM micrographs of a) CB_{lp}-260, b) CB_{lp}-280, c) CB_{lp}-300 and d) H-CB_{lp}.

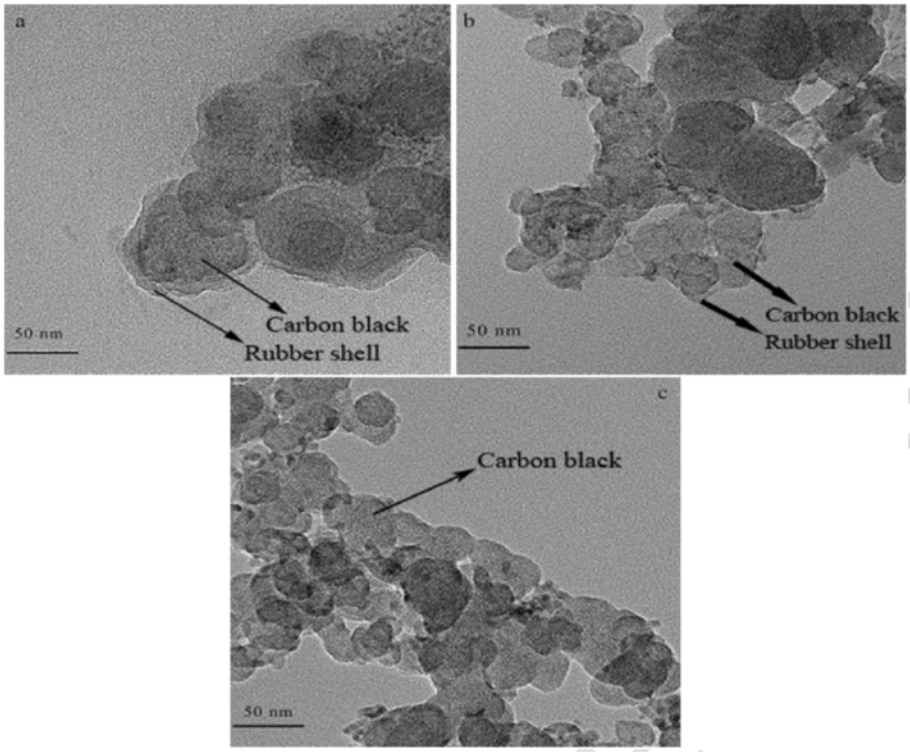

Fig. 3. TEM micrographs of a) CB_{lp}-280, b) CB_{lp}-300, c) H-CB_{lp}.

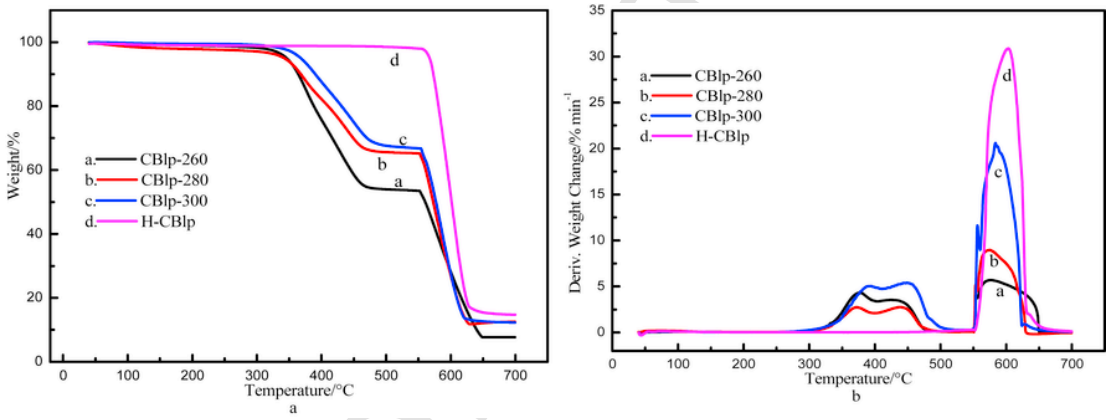

Fig. 4. TGA (a) and DTG (b) curves of CB_{lp}-260, CB_{lp}-280, CB_{lp}-300 and H-CB_{lp}.

Table 1
The maximum decomposition temperatures of CB_{lp}-260, CB_{lp}-280 and CB_{lp}-300 at different stages.

Carbon black	T_0/°C	T_{max1}/°C	T_{max2}/°C
CB_{lp}-260 °C	320	375	423
CB_{lp}-280 °C	316	373	438
CB_{lp}-300 °C	339	394	449

weight loss of E-CB_{lp}-300 is approximately 17.2 wt%, which was lower than the CB_{lp}-300 at 24.5 wt%, while the weight loss of E-CB_{lp}-280 is 29.2 wt %, slightly lower than that of CB_{lp}-280 at 31.2 wt%. In addition, the weight loss of E-CB_{lp}-260 is similar to the sample before solvent extraction. This finding indicates that the CB_{lp}-260 are still wrapped in a crosslinked rubber network consisting of primary bound rubber and partially destroyed loosely bound rubber (as shown in Fig. 2(a)), which could not be extracted by toluene at 130 °C. For CB_{lp}-280, the rubber shell primarily includes primary bound rubber and loosely bound rubber, the free-network chain structure is partially damaged at the elevated temperature (Fig. 3(b)). For CB_{lp}-300, more bound rubber layers are damaged (Fig. 3(c)) at 300 °C. As a result, the structure and composition of the rubber shell can be tailored to specific applications by varying the light pyrolysis temperature.

3.3. Physicochemical properties

XPS is applied to determine the surface properties and composition of the carbon black samples. The elemental compositions of CB_{lp}-260, CB_{lp}-280, CB_{lp}-300 and H-CB_{lp} are presented in Table 2.

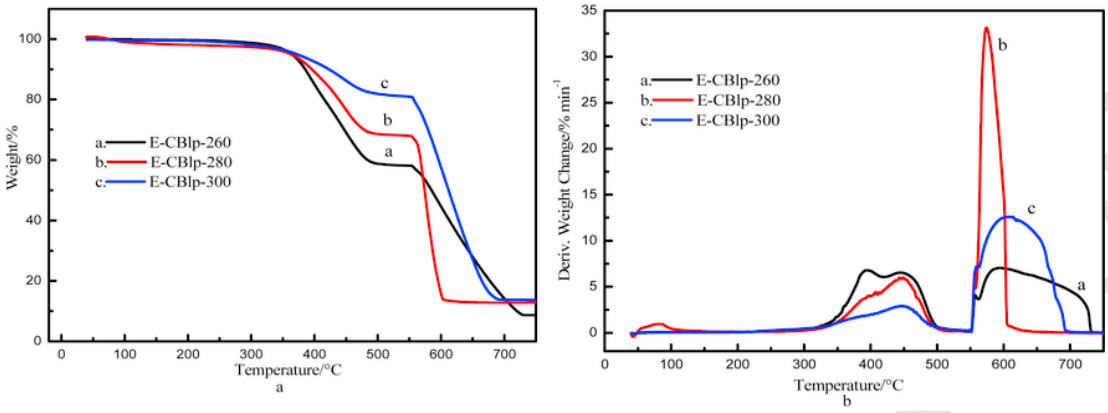

Fig. 5. TGA (a) and DTG (b) curves of E-CB_{lp} obtained at 260, 280, and 300 °C.

Table 2
Surface composition of CB_{lp}-260, CB_{lp}-280, CB_{lp}-300 and H-CB_{lp} as characterized by XPS.

Carbon black	Surface composition XPS (at %)				
	C	O	S	Zn	N
CB_{lp}-260	89.13	5.96	1.89	3.02	0
CB_{lp}-280	87.01	5.28	2.86	4.02	0.82
CB_{lp}-300	85.96	5.43	3.09	4.31	1.21
H-CB_{lp}	76.48	6.03	3.94	8.76	1.63

The elements S, Zn and N are detected from the carbon black samples, which are most likely from the curing additives in the rubber compounds [32]. Higher contents of the elements are detected for the samples treated with higher temperatures, reflecting more additives exposed at the surface of the CB_{lp} due to an increase in the damaged or destroyed crosslinked rubber structures at higher temperature [15,33].

The curve fitting of the C_{1s} peaks from the XPS spectrum are shown in Fig. 6. The XPS spectrum of C_{1s} for CB_{lp}-260, CB_{lp}-280, CB_{lp}-300 and H-CB_{lp} are fitted to four peaks: C—C or C—H (C_1, BE = 284.8 eV), C—O (C_2, BE = 285.5 eV), C═O (C_3, BE = 286.7 eV), and COOH (C_4, BE = 289.0 eV) [34–36]. The results of the curve-fitting of the C_{1s} spectrum are summarized in Table 3. As shown in Table 3, the COOH peak is not observed in the spectra of CB_{lp}-260 and CB_{lp}-280, which is due to the surface coverage of CB_{lp} by the crosslinked rubber and bound rubber. The bound rubber layer around CB_{lp}-300 is thinner than that on the surface of CB_{lp}-260 and CB_{lp}-280, as shown in Fig. 3 (b) and (c), which enables the —COOH to be detected by XPS. In addition, the increase of the content

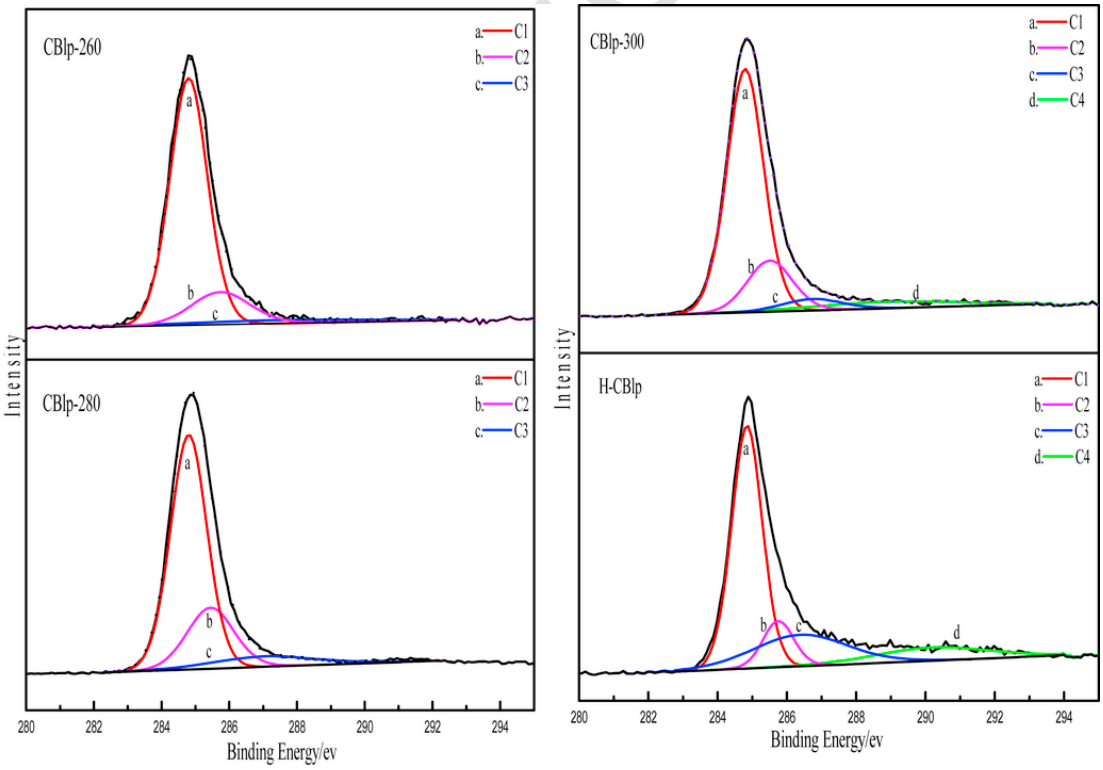

Fig. 6. C_{1s} XPS spectrum of carbon black CB_{lp}-260, CB_{lp}-280, CB_{lp}-300 and H-CB_{lp}.

Table 3
Area of the C_{1s} peaks of CB_{lp}-260, CB_{lp}-280, CB_{lp}-300 and H-CB_{lp}.

Compound	Area of C_{1s} peaks/at%			
	C_1(C—H or C—C)	C_2(C—O)	C_3(C=O)	C_4(COOH)
CB_{lp}-260	78.76	16.20	5.04	0
CB_{lp}-280	68.53	22.09	8.48	0
CB_{lp}-300	69.37	17.90	5.29	7.44
H-CB_{lp}	55.93	11.31	10.62	22.13

of C—O and C=O are clearly detected in CB_{lp}-280. This phenomenon is attributed to the rubber chains and some low molecular compounds being formed during reclaiming at 280 °C, which are more readily oxidized during the light pyrolysis process than the bound rubber shell of CB_{lp}-260 and CB_{lp}-300.

The graphitization structure of the CB_{lp}-260, CB_{lp}-280, CB_{lp}-300 and H-CB_{lp} samples were characterized using laser Raman spectroscopy. The original Raman spectra of CB_{lp}-260, CB_{lp}-280, CB_{lp}-300 and H-CB_{lp} samples and the four spectra with two bands fitting that were used for quantitative spectra analysis are shown in Fig. 7, and the fitting results are summarized in Table 4. Two relatively broad bands can be observed in the Raman spectra. The G-band at 1580 cm^{-1} is attributed to the presence of a graphitic structure and the D-band at ~1350 cm^{-1} is attributed to the amorphous carbon [26,37,38]. As shown in Fig. 7, with the increase in the extrusion temperature, the G peak exhibits a red shift (to lower wavenumbers) with an increase in the corresponding full width at half-maximum (FWHM). The intensity ratios of D and G bands (I_D/I_G) decrease from 1.03 to 0.86 with the increase in the extrusion temperature, indicating more graphitic structure is formed in the CB_{lp} at higher extrusion temperatures. The FWHM of the D band reflects the outer edge of the aromatic structure of carbon [39]. The highest FWHM of CB_{lp}-280 among the four samples suggests more free benzene rings introduced by the SBR chains around CB_{lp}-280 [26].

The distribution of particle sizes of CB_{lp}-280, CB_{lp}-300 and H-CB_{lp} in toluene is shown in Fig. 8. The average particle size of CB_{lp}-280 is 31 nm, which is 6.7% higher than that of CB_{lp}-300. The BET specific surface area of CB_{lp}-280 is 4.4 $m^2\ g^{-1}$, which is 73% smaller than that of CB_{lp}-300 (Table 5). The CB_{lp}-280 with more free rubber chains on the surface of the bound rubber layer leads to a larger average particle size with lower specific surface area [40] as compared to the CB_{lp}-300. the polydispersity index (PDI) of the samples shows that the H-CB_{lp} has the most uniform distribution, which is in agreement with the results as discussed in Figs. 2 and 3.

4. Conclusions

Core-shell structured CB_{lp} particles were derived from waste tire rubber via a reactive extrusion process. The structure and composition of the separated carbon black from tire rubber at three different pyrolysis temperatures were characterized.

The TEM observations and TGA analysis revealed that there are primary and destroyed loosely bound rubber existing on the surface of CB_{lp}-300, while the rubber shell of CB_{lp}-280 includes primary bound rubber, loosely bound rubber and some free rubber chains. The three-dimensional crosslinked rubber network on the surface of CB_{lp}-

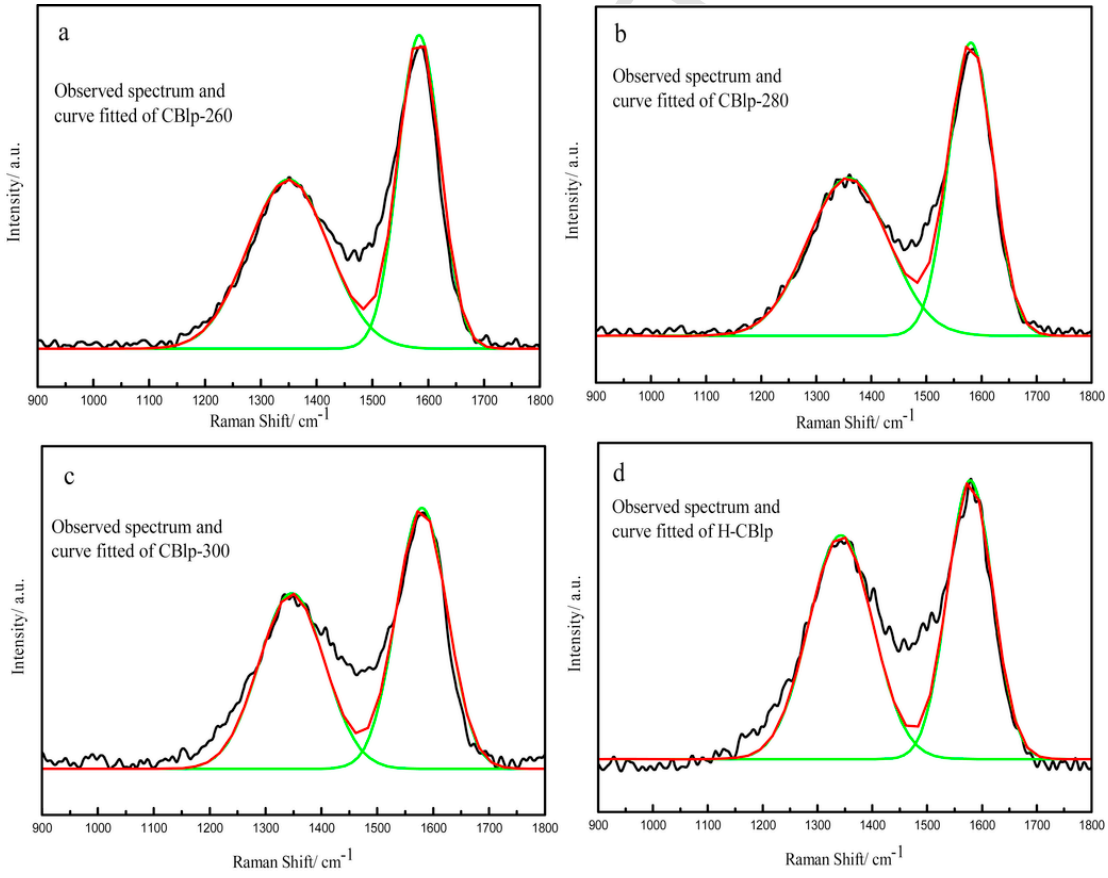

Fig. 7. Original Raman spectra of CB_{lp}-260, CB_{lp}-280, CB_{lp}-300 and H-CB_{lp} and the corresponding two spectra with two band fitting results.

Table 4
Fitting Raman spectra of CB_{lp}-260, CB_{lp}-280, CB_{lp}-300 and H-CB_{lp}.

Carbon black	G bands/cm^{-1}		D bands/cm^{-1}		I_D/I_G
	Position	FWHM	Position	FWHM	
CB_{lp}-260 °C	1584	89	1349	170	1.03
CB_{lp}-280 °C	1580	95	1358	173	0.97
CB_{lp}-300 °C	1578	108	1347	138	0.86
H-CB_{lp}	1579	98	1343	138	1.13

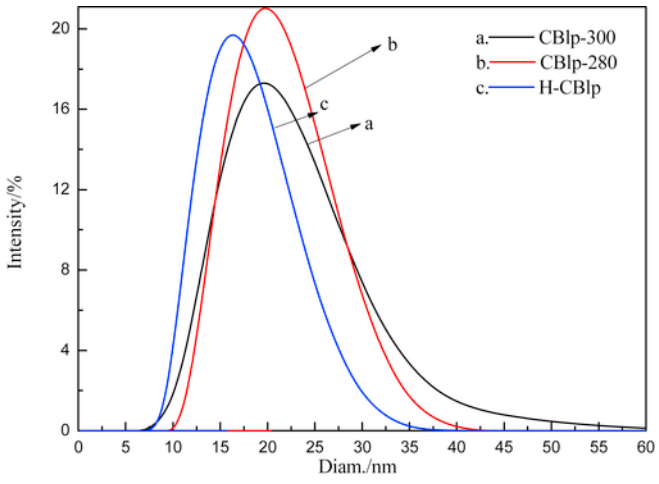

Fig. 8. Particle size distribution of CB_{lp}-280, CB_{lp}-300 and H-CB_{lp}.

Table 5
Particle size distribution and BET of CB_{lp}-280, CB_{lp}-300 and H-CB_{lp}.

Carbon black	Z-Average (r.nm)	PDI	BET surface area/m^2g^{-1}
CB_{lp}-280	31	0.26	4.40
CB_{lp}-300	28	0.29	16.37
H-CB_{lp}	24	0.24	76.63

260 is well-preserved during the extrusion process. The structure of CB_{lp} is affected by the composition and thickness of the rubber shell. The samples treated with higher temperatures exposed more additives to the surface of the CB_{lp} and exhibited higher contents of S, Zn and N. The average particle size of CB_{lp} increased with a decrease in the special surface area as the extrusion temperature was reduced. This reflects the effect of the extrusion temperature on the structure of the rubber shell.

This study demonstrates the interfacial interactions of carbon black with the rubber matrix by illustrating the structural change of bound rubber layers at different extrusion temperatures, and also provides a facile route for recycling waste tire rubbers into useful products.

Acknowledgements

This research is supported by an International cooperation project (No. 2013DFR50550) and Natural Science Foundation of China (No. 51273110).

References

[1] I. Hita, M. Arabiourrutia, M. Olazar, J. Bilbao, J.M. Arandes, P.C. Sánchez, Opportunities and barriers for producing high quality fuels from the pyrolysis of scrap tires, Renew. Sustain. Energy Rev. 56 (2016) 745–759.
[2] V. Gupta, B. Gupta, A. Rastogi, S. Agarwal, A. Nayak, A comparative investigation on adsorption performances of mesoporous activated carbon prepared from waste rubber tire and activated carbon for a hazardous azo dye—Acid Blue 113, J. Hazard. Mater. 186 (1) (2011) 891–901.
[3] J.D. Martínez, N. Puy, R. Murillo, T. García, M.V. Navarro, A.M. Mastral, Waste tyre pyrolysis–a review, Renew. Sustain. Energy Rev. 23 (2013) 179–213.
[4] S. Ramarad, M. Khalid, C. Ratnam, A.L. Chuah, W. Rashmi, Waste tire rubber in polymer blends: a review on the evolution, properties and future, Prog. Mater. Sci. 72 (2015) 100–140.
[5] T.A. Saleh, G.I. Danmaliki, Adsorptive desulfurization of dibenzothiophene from fuels by rubber tyres-derived carbons: kinetics and isotherms evaluation, Process Saf. Environ. Prot. 102 (2016) 9–19.
[6] A. Undri, S. Meini, L. Rosi, M. Frediani, P. Frediani, Microwave pyrolysis of polymeric materials: waste tires treatment and characterization of the value-added products, J. Anal. Appl. Pyrolysis 103 (2013) 149–158.
[7] M. Gągol, G. Boczkaj, J. Haponiuk, K. Formela, Investigation of volatile low molecular weight compounds formed during continuous reclaiming of ground tire rubber, Polym. Degrad. Stab. 119 (2015) 113–120.
[8] X. Guo, D. Xiang, G. Duan, P. Mou, A review of mechanochemistry applications in waste management, Waste Manag. 30 (1) (2010) 4–10.
[9] K. Formela, M. Kleinb, X. Colomc, M.R. Saebd, Investigating the combined impact of plasticizer and shear force on the efficiency of low temperature reclaiming of ground tire rubber (GTR), Polym. Degrad. Stab. 125 (2016) 1–11.
[10] J. Aguado, D. Serrano, J. Escola, Fuels from waste plastics by thermal and catalytic processes: a review, Industrial Eng. Chem. Res. 47 (21) (2008) 7982–7992.
[11] G.-G. Choi, S.-H. Jung, S.-J. Oh, J.-S. Kim, Total utilization of waste tire rubber through pyrolysis to obtain oils and CO 2 activation of pyrolysis char, Fuel Process. Technol. 123 (2014) 57–64.
[12] G. López, M. Olazar, R. Aguado, J. Bilbao, Continuous pyrolysis of waste tyres in a conical spouted bed reactor, Fuel 89 (8) (2010) 1946–1952.
[13] T.A. Saleh, V.K. Gupta, Processing methods, characteristics and adsorption behavior of tire derived carbons: a review, Adv. Colloid Interface Sci. 211 (2014) 93–101.
[14] A. Undri, B. Sacchi, E. Cantisani, N. Toccafondi, L. Rosi, M. Frediani, P. Frediani, Carbon from microwave assisted pyrolysis of waste tires, J. Anal. Appl. Pyrolysis 104 (2013) 396–404.
[15] P.T. Williams, Pyrolysis of waste tyres: a review, Waste Manag. 33 (8) (2013) 1714–1728.
[16] H. Yamazaki, T. Nagasawa, W. Choi, T. Endo, Transformation of vulcanized natural rubber into lower molecular weight polymers and their application to grafted copolymer synthesis with some vinyl monomers, J. Appl. Polym. Sci. 101 (6) (2006) 4003–4010.
[17] J. Shi, H. Zou, L. Ding, X. Li, K. Jiang, T. Chen, X. Zhang, L. Zhang, D. Ren, Continuous production of liquid reclaimed rubber from ground tire rubber and its application as reactive polymeric plasticizer, Polym. Degrad. Stab. 99 (2014) 166–175.
[18] C. Nah, J.Y. Lim, B.H. Cho, C.K. Hong, A.N. Gent, Reinforcing rubber with carbon nanotubes, J. Appl. Polym. Sci. 118 (3) (2010) 1574–1581.
[19] J. Fröhlich, W. Niedermeier, H.-D. Luginsland, The effect of filler–filler and filler–elastomer interaction on rubber reinforcement, Compos. Part A Appl. Sci. Manuf. 36 (4) (2005) 449–460.
[20] V. Litvinov, R. Orza, M. Kluppel, M. Van Duin, P. Magusin, Rubber–filler interactions and network structure in relation to stress–strain behavior of vulcanized, carbon black filled EPDM, Macromolecules 44 (12) (2011) 4887–4900.
[21] D. Gabriel, A. Karbach, D. Drechsler, J. Gutmann, K. Graf, S. Kheirandish, Bound rubber morphology and loss tangent properties of carbon-black-filled rubber compounds, Colloid Polym. Sci. (2015) 1–11.
[22] S.-S. Choi, E. Ko, Novel test method to estimate bound rubber formation of silica-filled solution styrene-butadiene rubber compounds, Polym. Test. 40 (2014) 170–177.
[23] S. Li, C. Wan, X. Wu, S. Wang, Core-shell structured carbon nanoparticles derived from light pyrolysis of waste tires, Polym. Degrad. Stab. 129 (2016) 192–198.
[24] Y. Hoshikawa, B. An, S. Kashihara, T. Ishii, M. Ando, S. Fujisawa, K. Hayakawa, S. Hamatani, H. Yamada, T. Kyotani, Analysis of the interaction between rubber polymer and carbon black surfaces by efficient removal of physisorbed polymer from carbon-rubber composites, Carbon 99 (2016) 148–156.
[25] S. Saiwari, W. Dierkes, J. Noordermeer, Devulcanization of whole passenger care tire material, KGK Kautsch. Gummi, Kunstst. 66 7–8 (2013) (2013) 20–25.
[26] S. Jin, Q. Li, C. Wu, Encapsulation of surface-modified carbon blacks by poly (sodium-p-styrenesulfonate) via a phase separation method, Powder Technol. 279 (2015) 173–178.
[27] D. Borah, S. Satokawa, S. Kato, T. Kojima, Characterization of chemically modified carbon black for sorption application, Appl. Surf. Sci. 254 (10) (2008) 3049–3056.

[28] K.A. Dubkov, S.V. Semikolenov, D.P. Ivanov, D.E. Babushkin, V.D. Voronchikhin, Scrap tyre rubber depolymerization by nitrous oxide: products and mechanism of reaction, Iran. Polym. J. 23 (11) (2014) 881–890.
[29] A. Nadal Gisbert, J. Crespo Amoros, J. López Martínez, A.M. Garcia, Study of thermal degradation kinetics of elastomeric powder (ground tire rubber), Polymer-Plastics Technol. Eng. 47 (1) (2007) 36–39.
[30] B. Zhang, Y. Chen, F. Wang, R. Hong, Surface modification of carbon black for the reinforcement of polycarbonate/acrylonitrile–butadiene–styrene blends, Appl. Surf. Sci. 351 (2015) 280–288.
[31] J.L. Leblanc, Rubber–filler interactions and rheological properties in filled compounds, Prog. Polym. Sci. 27 (4) (2002) 627–687.
[32] M. Bernardo, N. Lapa, M. Gonçalves, B. Mendes, F. Pinto, I. Fonseca, H. Lopes, Physico-chemical properties of chars obtained in the co-pyrolysis of waste mixtures, J. Hazard. Mater. 219 (2012) 196–202.
[33] X. Zhang, T. Wang, L. Ma, J. Chang, Vacuum pyrolysis of waste tires with basic additives, Waste Manag. 28 (11) (2008) 2301–2310.
[34] A. Attout, S. Yunus, P. Bertrand, Electrospinning and alignment of polyaniline-based nanowires and nanotubes, Polym. Eng. Sci. 48 (9) (2008) 1661–1666.
[35] H. Darmstadt, C. Roy, S. Kaliaguine, Characterization of pyrolytic carbon blacks from commercial tire pyrolysis plants, Carbon 33 (10) (1995) 1449–1455.
[36] Y. Wu, S. Wen, J. Shen, J. Jiang, S. Hu, L. Zhang, L. Liu, Improved dynamic properties of natural rubber filled with irradiation-modified carbon black, Radiat. Phys. Chem. 111 (2015) 91–97.
[37] K. Rao, A. Chaudhary, F. Yehya, Investigation of solid carbon blacks using pulsed photoacoustic and double resonant Raman spectroscopy for the identification of trinitrotoluene, Sensors Actuators B Chem. 231 (2016) 830–836.
[38] N. Larouche, B.L. Stansfield, Classifying nanostructured carbons using graphitic indices derived from Raman spectra, Carbon 48 (3) (2010) 620–629.
[39] A.C. Ferrari, J. Robertson, Interpretation of Raman spectra of disordered and amorphous carbon, Phys. Rev. B 61 (20) (2000) 14095.
[40] J. Qi, N. Benipal, D.J. Chadderdon, J. Huo, Y. Jiang, Y. Qiu, X. Han, Y.H. Hu, B.H. Shanks, W. Li, Carbon nanotubes as catalysts for direct carbohydrazide fuel cells, Carbon 89 (2015) 142–147.